Current Biology *17*, 1349–1355, August 7, 2007 DOI 10.1016/j.cub.2007.06.067

Report

The Role of the Actomyosin Cytoskeleton in Coordination of Tissue Growth during *Drosophila* Oogenesis

Ying Wang[1] and Veit Riechmann[1,*]
[1] Institut für Entwicklungsbiologie
Universität zu Köln
Gyrhofstr.17
D-50931 Köln
Germany

Summary

The *Drosophila* egg chamber is an organ composed of a somatic epithelium that covers a germline cyst. After egg-chamber formation, the germline cells grow rapidly without dividing while the surface of the epithelium expands by cell proliferation [1, 2]. The mechanisms that coordinate growth and morphogenesis of the two tissues are not known. Here we identify a role for the actomyosin cytoskeleton in this process. We show that myosin activity is restricted to the epithelium's apical surface, which is facing the growing cyst. We demonstrate that the epithelium collapses in the absence of myosin activity and show that the force that deforms the epithelium originates from the growing cyst. Thus, myosin activity maintains epithelial shape by balancing the force emanating from cyst growth. Further, our data indicate that cyst growth induces cell division in the epithelium. In addition, we show how apical restriction of myosin activity is controlled. Myosin is activated at the apical cortex by localized Rho kinase and inhibited at the basolateral cortex by PP1β9C. In addition, our data indicate that active myosin is apically anchored by the Baz/Par-6/aPKC complex.

Results and Discussion

To analyze the correlation between cyst growth and follicle cell division, we counted dividing cells in the follicular epithelium. Within the first 56 hr that are required to form a stage 3 egg chamber, cell-division rates are very low. In the 14 hr period between stage 4 and stage 6, however, cell-division rates continuously increase (Table 1). We calculate that during this time, the volume of the cyst increases approximately 11-fold. This parallel increase in mitosis and cyst growth reflects how the growth of the inner cyst is compensated by cell division in the outer follicular epithelium. After stage 7, the follicle cells stop dividing and undergo diverse morphological changes (reviewed in [1, 2]).

Newly formed egg chambers are round and change their shape to ellipsoid during early oogenesis. After stage 7, the process of egg-chamber elongation, which is mediated by a polarized actin cytoskeleton within the follicular epithelium, starts. Actin fibers at the basal cortex of the follicle cells run perpendicular to the anterior-posterior axis of the egg chamber, and their contraction leads to an axis expansion [3–5]. The mechanisms that shape the egg chamber before elongation takes place are unknown. The simultaneous and rapid growth of cyst and epithelium after stage 3 indicates that the development of the two tissues is precisely coordinated. It is, however, unclear how epithelial morphogenesis and proliferation are coupled to the growth of the cyst.

Spatial Restriction of Myosin Activity in the Follicular Epithelium

The actin cytoskeleton is central for the cell shape, and is thus a possible candidate involved in a controlled epithelial response to the cyst growth. We examined the activity in the actomyosin cytoskeleton by using an antibody specific for the activated form of the regulatory light chain of nonmuscle myosin II (RMLC). The phospho-specific RMLC antibody binds to pSer21 and reveals myosin in its active state [6, 7]. Around stage 3 of oogenesis, myosin activity restricts to the apical cortex of the follicle cells, where it is maintained until late oogenesis (Figures 1B–1E). After stage 7, myosin activity is also present at the basal cortex of the follicle cells in the actin bundles required for egg chamber elongation (Figures 1E and 1F) [3–5]. Optical confocal sections reveal a pattern of myosin activity in these long parallel bundles that is reminiscent of stress fibers (Figure 1F). In contrast, at the apical cortex, myosin is active in short fibers with random orientation reminiscent of a web (Figure 1G).

Apical Restriction of Myosin Activity Is Dependent on the Baz/Par-6/aPKC Complex

The membrane domains of the follicle cells are established before myosin activity restricts to the apical cortex at stage 3 [8]. To examine how apical myosin activation relates to follicle cell polarity, we analyzed mutants affecting epithelial polarity. To avoid perdurance of the wild-type protein after clone induction, we focused on large clones, or clones spanning the whole epithelium. The adherence junctions are central for the organization of the apical actin cytoskeleton, and the domain of myosin activity extends into the region where they localize (Figure 1D). We therefore examined null mutants of *armadillo* (*arm*), which encodes *Drosophila* β-catenin. It has previously been shown that the adherence junctions are disrupted in *arm* follicle cell clones as neither DE- or DN-cadherin are detectable [8]. As a result, *arm* mutant cells exhibit strong cell-shape defects [8, 9]. Surprisingly, we found that myosin activity is clearly restricted to the apical membrane in *arm* follicle cell clones (Figure 2B). Thus, myosin activity restricts apically in the absence of adherence junctions.

The apical membrane domain is established by the Crumbs (Crb)/Stardust (Sdt)/Patj complex and the Bazooka (Baz)/Par-6/aPKC complex. All these proteins localize, like pRMLC, to the apical membrane of the follicular epithelium [8, 10, 11]. In epithelia lacking *crb*,

*Correspondence: veit.riechmann@uni-koeln.de

Table 1. Number of Phospho-Histone H3-Positive Cells at Different Stages of Oogenesis

	Germarium	Stage 2	Stage 3	Stage 4	Stage 5	Stage 6
Wild-type	0.5 ± 1.14 (n = 42)	1.1 ± 1.31 (n = 34)	2.2 ± 2.04 (n = 35)	6.2 ± 3.25 (n = 36)	12.3 ± 4.26 (n = 29)	21.3 ± 5.69 (n = 34)
sqh^{AX}	n.d.	n.d.	n.d.	2.5 ± 2.66 (n = 11)	7.9 ± 5.65 (n = 21)	10.5 ± 9.33 (n = 15)
rok^{2}	n.d.	n.d.	n.d.	6.6 ± 3.5 (n = 9)	13 ± 5.03 (n = 10)	19.5 ± 5.04 (n = 13)
dia^{5}	n.d.	n.d.	n.d.	2.8 ± 2.12 (n = 8)	6.2 ± 4.02 (n = 16)	14.6 ± 6.02 (n = 19)
ovo^{D1}	0.5 ± 0.82 (n = 69)	1.1 ± 1.3 (n = 38)	2.6 ± 1.23 (n = 29)	3.1 ± 2.76 (n = 48)	5 ± 3.07 (n = 44)	2.4 ± 3.08 (n = 55)

Wild-type ovaries or ovaries in which homozygous clones of the indicated mutation had been induced were stained with a phospho-Histone H3 antibody. The ovaries were also stained with DAPI to visualize nuclei and, in the case of the mutants, with anti-GFP or β-galactosidase. The stages of the egg chambers were determined by their position within the ovariole, by the size of the egg chamber, and by the size of the oocyte (see [1, 27] for stages of oogenesis). The total number of phospho-Histone H3 positive cells in the whole epithelium of a given ovary were counted. Only those egg chambers in which the clones covered approximately one quarter or more of the follicular epithelium were analyzed. For the *ovo*^{D1} counting, progeny from the cross performed to induce *sqh* clones were taken. From this cross, we analyzed females, which carry the FM6 balancer instead of the *sqh* muation. "n.d." indicates not determined.

myosin restriction is affected as revealed by the interrupted apical pRMLC pattern (arrows in Figure 2C) and by ectopic activity at the basal membrane (arrowheads). However, apical myosin activity is not completely disrupted as broad regions of the epithelium still concentrate higher levels of pRMLC at the apical compared to the basal cortex. In contrast, *par-6*, *aPKC* and *baz* mutants abolish the formation of the apical myosin activity. In these mutants, apical pRMLC restriction is lost, and ectopic myosin activity is detectable in the cytoplasm and at the basal cortex (Figures 2D–2F). To test whether the two apical complexes cooperate in apical myosin restriction, we examined *baz sdt* double mutants. The phenotype of the double mutants is, however, very similar to that of the *baz* single mutants (Figure S1A in the Supplemental Data available online), suggesting that apical myosin activity is controlled by the Baz/Par-6/aPKC complex.

To further analyze this interaction, we immunoprecipitated the Baz/Par-6/aPKC complex from ovaries using an antibody against Baz. Western-blot analysis of the precipitated protein complex reveals a strong enrichment of Baz and aPKC. Notably, pRMLC is also present in the precipitated protein complex, indicating an association of Baz and active myosin (Figure 2G). Taken together, our genetic data show that *baz*, *par-6*, and *aPKC* are required for apical myosin restriction, and our biochemical data show that Baz associates with pRMLC. This suggests the Baz/Par-6/aPKC complex anchors active myosin at the apical cortex. To further analyze the role of the complex in the apical restriction of myosin activity, we examined its localization in mutants that affect pRMLC localization. Consistent with a function in the anchoring of active myosin, we found that apical aPKC localization is not affected in *arm* mutants (Figure S1B), in which pRMLC is apically restricted. Further, apical aPKC localization is interrupted in *crb* mutants (Figure S1C), in which pRMLC localization is also interrupted. In summary, our data suggest that the Baz/Par-6/aPKC complex anchors active myosin at the apical cortex independently of the adherence junctions.

PP1β9C Prevents Basal and Lateral Myosin Activity

To examine how myosin activity is inhibited during early oogenesis at the basal and lateral cortex, we analyzed the localization and function of PP1β9C, the phosphatase that deactivates phosphorylated RMLC [12]. In follicle cells, PP1β9C is ubiquitously distributed as revealed by a hemagglutinin (HA) fusion protein (Figure S2C). PP1β9C is encoded by *flap wing* (*flw*). Western-blot analysis of the viable *flw*^{1} allele showed that the total pRMLC levels in ovaries are increased 2.8-fold compared to those of the wild-type (Figure S2A). The total increase is the result of ectopic myosin activity in the follicular epithelium. This is revealed by *flw*^{6} follicle cell clones and homozygous *flw*^{1} mutant egg chambers, which show pRMLC staining at the basal and lateral cortex (Figures S2B and S2G). Interestingly, the ectopic Myosin activity is accompanied by an irregular and wavy appearance of the apical surface of the epithelium (Figures S2E and S2G). In addition, *flw* mutant egg chambers are not round or ellipsoid like the wild-type but are either stretched or develop bulges (Figures S2B, S2E, and S2G). The coincidence of the altered shape with the ectopic pRMLC staining in the follicular epithelium suggests that the abnormal shape is the result of ectopic myosin activity. This is confirmed by the finding that the expression of constitutively active RMLC results in a very similar phenotype (Figure S2I). The defects in *flw* mutants are not secondary effects of mislocalization of the Baz/Par-6/aPKC complex as the localization of aPKC is indistinguishable from that of the wild-type (Figures S2D and S2E). In summary, these results show that PP1β9C activity is required to prevent myosin activity at the basal and lateral cortex. They further suggest that during early oogenesis, myosin activity has to be restricted to the apical cortex to ensure the development of normally shaped egg chambers.

Localized Rok Activates Myosin at the Apical Cortex of the Follicular Epithelium

To investigate how myosin is activated at the apical cortex, we analyzed the function of Rok, which has been shown to regulate myosin phosphorylation [13–15]. Myosin phosphorylation is greatly reduced but still detectable in *rok* mutant follicle cell clones (Figure 3B). This confirms that Rok phosphorylates myosin in the follicular epithelium, but also indicates that Rok is not the only kinase involved in myosin activation. A HA-Rok fusion protein accumulates in particles at the apical cortex of the follicle cells, which are in close proximity to the web-like myosin fibers (Figures S1D and S1E). Thus, localized Rok activates myosin in the follicular epithelium.

Because RMLC phosphorylation is strongly reduced in *rok* mutant cells, we used *rok* clones to examine the

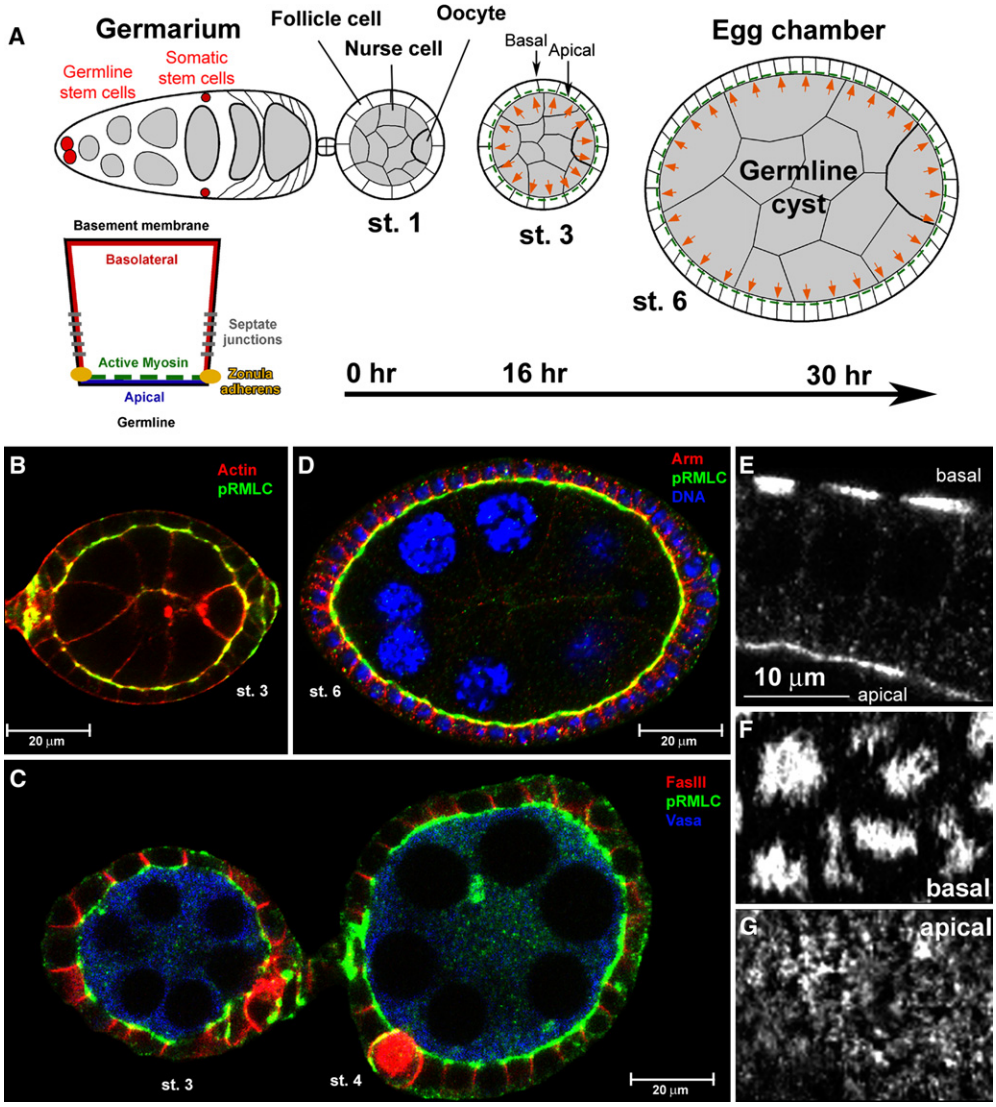

Figure 1. Oogenesis and Follicle Cell Development

Egg chambers are oriented such that anterior is to the left and posterior is to the right.

(A) Schemes depict egg-chamber development and a polarized follicle cell.

(B) Stage 3 egg chamber stained for actin (red) and pRMLC (green). The yellow overlap at the apical site of the follicular epithelium indicates the formation of the apical restriction of myosin activity.

(C) Two egg chambers stained for the lateral marker FasIII (red) and pRMLC (green). Vasa (blue) highlights the germline cyst.

(D) Stage 6 egg chamber stained for pRMLC and Arm to mark the adherence junctions. The shape of the cyst has changed from round to ellipsoid.

(E–G) pRMLC localization in a stage 10a egg chamber. A sagittal section through three follicle cells is shown (E). Myosin activity at the basal and apical cortex of the follicular epithelium is visible. Confocal sections at the apical and basal cortex of the follicular epithelium reveal different patterns of Myosin activity (F and G).

function of apical myosin activity. *rok* mutant follicle cells divide normally (Table 1), form a monolayered follicular epithelium (Figure 3I), and retain polarity (data not shown). However, *rok* mutant cells fail to adopt a normal shape. As a consequence, the epithelium is flatter in these regions than it is in regions with *rok* activity (Figures 3A, 3B, and 3I). Optical sections at the level of the zonula adherens show that *rok* mutant cells are also stretched compared to neighboring wild-type cells (Figure 3H). Furthermore, egg chambers with large follicle cell clones develop abnormal shapes as the cyst bulges outwards in the area of the clones (Figure 3; compare Figure 3I with Figure 3F, and see arrows in Figure 3I). These results show that *rok* is required for follicle cell and egg-chamber shape, and indicate that the function of the apical myosin activity is to prevent flattening and stretching of epithelial cells.

Apical Myosin Activity Is Required to Maintain Follicle Cell and Egg-Chamber Shape

To test the function of the apical myosin activity directly, we generated follicle cell clones using a null mutation for *spaghetti squash* (*sqh*). *sqh* encodes RMLC and was previously shown to be required for other aspects of

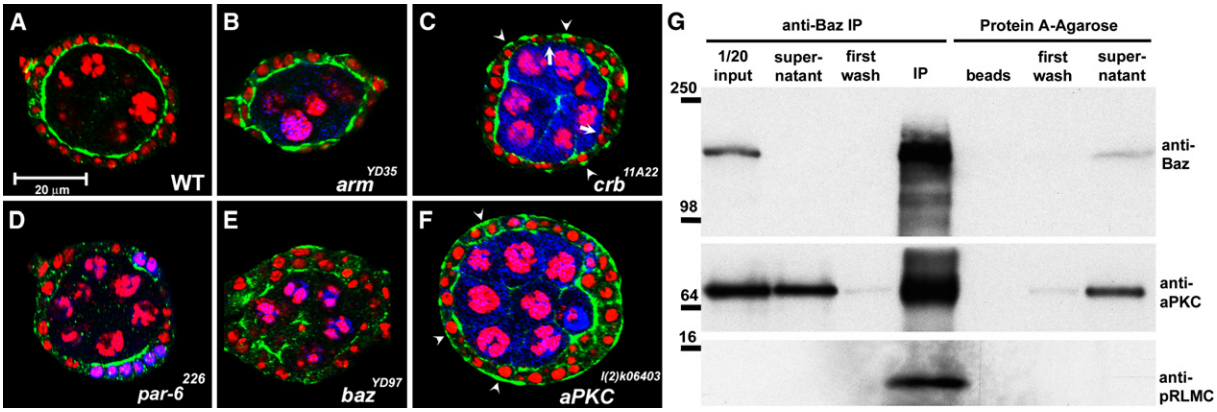

Figure 2. pRMLC Localization in Mutants Affecting Apical Polarity, and Coprecipitation of Baz and pRMLC

(A–F) Stage 4/5 egg chambers. A wild-type egg chamber shows apical restriction of pRMLC (green) (A). Egg chambers with follicle cell clones homozygous mutant for the indicated genes are shown (B–F). Clones are marked by the absence of either green fluorescent protein (GFP) (C and E) or β-Galactosidase (B, D, and F) shown in blue. In all egg chambers, the clones cover the whole follicular epithelium, with the exception of (D). Follicle cell clones mutant for a null allele of *arm* are shown in (B). Only very few large clones were obtained, all of which strongly affected the morphology of the epithelium. Nevertheless, pRMLC is restricted apically. In (C) and (F), arrowheads point to ectopic myosin activity at the basal cortex. Arrows indicate the absence of apical pRMLC in *crb* mutants. An egg chamber with two large *par-6* clones showing complete absence of pRMLC at the apical cortex is shown in (D). The few wild-type cells (blue) retain apical myosin activity.

(G) Immunoprecipitation of Baz from an ovarian extract. The western blot was incubated with the indicated antibodies, revealing that aPKC and pRMLC precipitate with Baz (left half). pRMLC, aPKC, and Baz did not bind to protein A agarose in the control experiment (right half). Experiments in which an antibody against the transcription factor Twist was used as a control gave the same result. The pRMLC signal is not visible in the input lane because of the short exposure time of the film shown.

egg-chamber morphogenesis, like cyst separation and follicle cell migration [16]. Follicle cells lacking RMLC activity are extremely flat and appear stretched (Figures 3A, 3C–3E). In many egg chambers with *sqh* clones, we found gaps in the follicular epithelium, suggesting that stretching of the follicle cells eventually disrupts the monolayer (Figure 3G). The flat *sqh* mutant cells retain polarity, as revealed by the localization of Discs large (Dlg), a marker for the region where the septate junctions are formed (Figure 3E), and the localization of the apical marker aPKC (Figure 3C). The change in the shape of the follicle cells is accompanied by a change in the morphology of the egg chamber. Although those regions of the egg chamber covered by wild-type follicle cells retain a normal shape, the germline cyst bulges out in regions covered by *sqh* mutant cells (Figures 3A, 3C–3E). In summary, the morphological defects in the *sqh* clones are very similar to the defects in the *rok* mutant clones, although the *sqh* phenotype is much stronger. The stronger morphological defects in *sqh* mutants are consistent with our finding that RMLC activity is only reduced in *rok*, whereas it is abolished in *sqh* mutant cells.

sqh function is also required for cytokinesis [6], and, consistent with this, epithelia with *sqh* mutant clones show a reduced number of phospho-Histone H3-positive cells (Table 1), huge nuclei, and abnormally large cells (arrows in Figures 3A and 3D). To examine whether these defects contribute to the morphological defects, we analyzed epithelia with clones mutant for *diaphanous* (*dia*), another gene required for cytokinesis [17]. Using the weak allele dia^5, we identified follicle cell clones showing cytokinesis defects in the presence of a normal actin cortex. During early oogenesis, these clones retain a rectangular shape, do not flatten, and the underlying cyst bulges out only very mildly (Figure 3A). Late clones show no outward bulging over the growing oocyte and maintain a normal cell shape, with the exception that the cells are bigger because of the absence of cytokinesis (Figure 3D). Thus, cytokinesis defects alone do not affect the rectangular shape of the follicle cells, and they affect the shape of the egg chamber only mildly and only during early oogenesis. Importantly, the morphological defects are fully penetrant in *sqh* mutant follicle cell clones. We therefore conclude that the morphological defects in egg chambers with *sqh* clones are the result of the loss of apical myosin activity.

Apical Myosin Activity Counteracts Forces Emanating from Cyst Growth

The epithelial deformations in *sqh* clones suggest a stress that is acting on the epithelium. The outward bulging of the cyst further suggests that the origin of this stress is the volume increase of the growing cyst. Wild-type cells might resist this stress because of the myosin activity at the apical cortex that is facing the cyst, whereas *sqh* mutant cells collapse. To test this hypothesis, we blocked cyst growth by using a chromosome carrying an ovo^{D1} mutation. ovo^{D1} is a dominant female-sterile mutation that is normally applied in germline mosaics. Importantly, the ovo^{D1} phenotype is restricted to the germline and does not affect the somatic epithelium [18]. The ovo^{D1} harbouring chromosome that we used in our experiment leads to a growth arrest after stage 4 resulting in small stage 6 egg chambers, which later degenerate (Figure 4C and data not shown).

We induced *sqh* follicle cell clones in parallel in wild-type and in ovo^{D1} mutant backgrounds and analyzed cyst and epithelial shape. Strikingly, *sqh* mutant follicle cells maintain their rectangular shape when cyst growth is blocked, whereas *sqh* cells are deformed when the cyst grows (compare arrow length in Figure 4C).

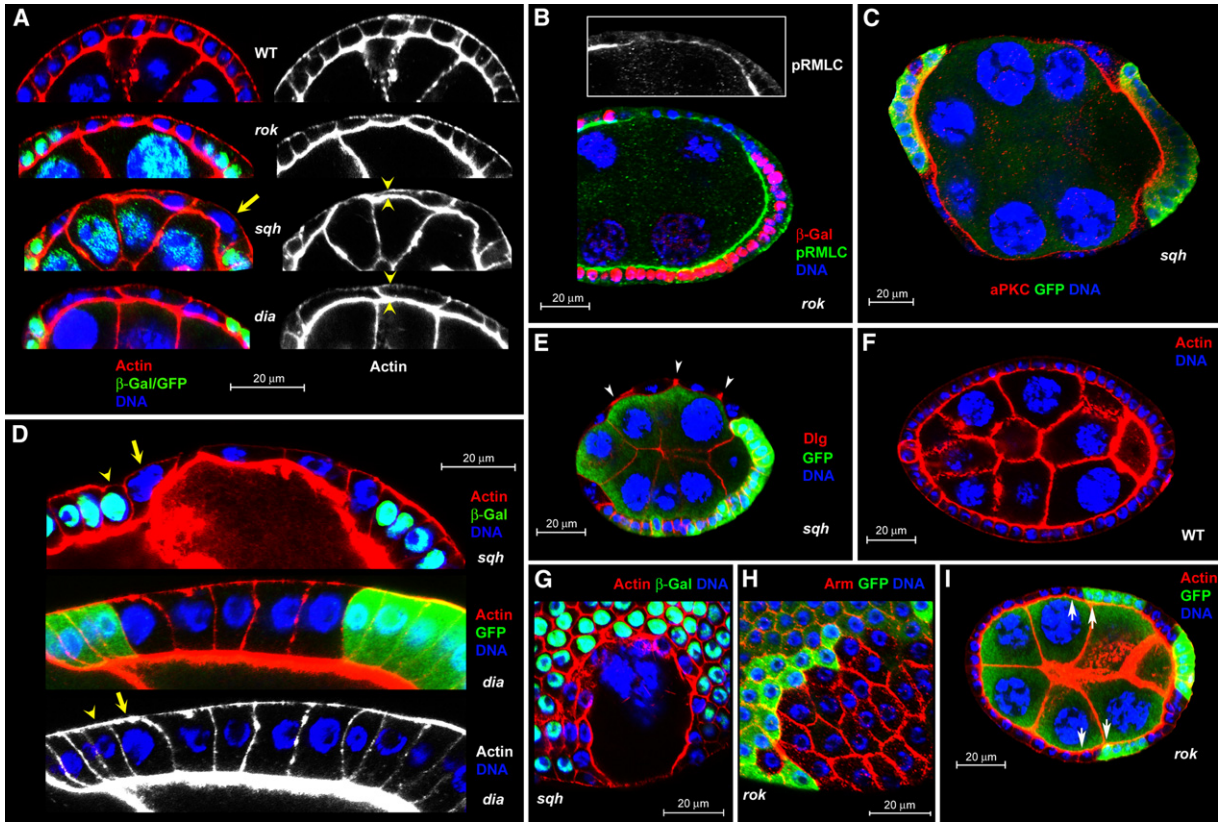

Figure 3. Morphological Defects in Egg Chambers with Homozygous *sqh* and *rok* Follicle Cell Clones

Stainings and genotypes of clones are indicated.

(A) Clones in the follicular epithelium of stage 5/6 egg chambers. Clones are marked by the absence of green in the left column. The right column shows actin cortex stained with phalloidin alone. The arrow marks an increased nucleus in a *sqh* mutant clone, indicating a failure in cytokinesis. The lower two panels compare *sqh* and *dia* clones, both spanning three cells with fused nuclei. Note that in the *sqh* clone, the central epithelial cell collapses (arrowheads), and the cyst bulges outward. This is in contrast to the *dia* clone, in which the central cell maintains its rectangular (arrowheads) shape and the cyst does not extrude significantly.

(B) Stage 7 egg chamber with a *rok* mutant follicle cell clone. The clone is marked by the absence of β-gal (red) in the nuclei. Coinciding with the clone border, pRMLC levels drop. The inset shows the pRMLC channel alone.

(C) *sqh* mutant cells are stretched but retain aPKC localization at the apical membrane. Clones are marked by the absence of green.

(D) Follicle cell clones in a stage 8 (up) and stage 9 (down) egg chambers mutant for *sqh* and *dia*. Clones are marked by the absence of green. The two lower pictures show the same egg chamber. Arrows mark mutant cells with increased nuclei due to cytokinesis defects, and arrowheads point toward wild-type nuclei.

(E) Lateral Dlg localization in the mutant cells (arrowheads) indicates the presence of septate junctions in a *sqh* mutant clone of a stage 6 egg chamber. Note the outward bulging of the cyst in regions where follicle cells are mutant.

(F) Wild-type stage 6 egg chamber showing a typical ellipsoid shape.

(G) Rupture of the follicular epithelium in a *sqh* mutant clone in a stage 8 egg chamber.

(H) Confocal section at the level of the adherence junctions of a stage 9 egg chamber. *rok* mutant cells stretch, whereas neighboring wild-type cells retain a normal shape.

(I) Stage 5/6 egg chamber with one large anteriorly located and two small posteriorly located *rok* mutant clones. Cells in the large clone are flat, whereas cells in small clones retain cuboidal shape to some extent. Note the irregular shape of the germline cyst and the outward bulging of the cyst (arrows).

Moreover, the cyst bulges out underneath the *sqh* clones only in the wild-type background, but not in the ovo^{D1} mutant cysts (arrows in Figures 4A and 4C). Thus, myosin activity is only required for epithelial and egg-chamber shape if the cyst is growing. We therefore conclude that epithelial myosin activity counteracts the force from the growing cyst.

How could myosin activity counteract stress from the growing cyst mechanistically? In *Dictyostelium*, it has been shown that the cell membrane is able to resist deformations induced by a cell poker, revealing stiffness of the cortex. In myosin mutants, the cortical stiffness is greatly reduced, indicating that stiffness is generated by myosin-mediated contractions within the actin cortex [19]. Consistent with this, in vitro studies demonstrated that myosin activity increases the stiffness of crosslinked actin filaments by a factor of 100 [20]. Stiffness is generated by diminishing thermal fluctuations within a crosslinked actin network [21]. Myosin is able to suppress these fluctuations by mediating contractions of actin filaments between crosslink points (Figures S3A and S3B). We propose that stiffness is a crucial feature of the apical epithelial cortex in response to the stress emanating from the growing cyst, and that myosin regulates the stiffness by generating tension between actin crosslink points.

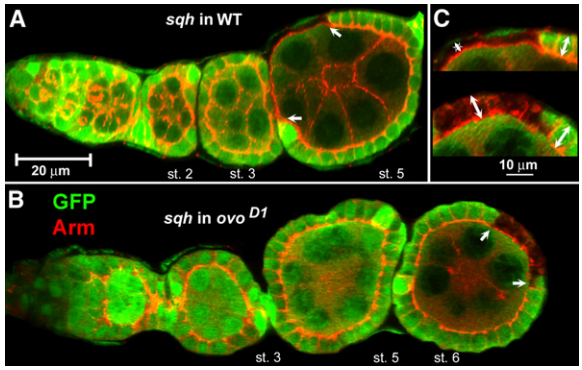

Figure 4. Block of Cyst Growth Suppresses Morphological Defects of *sqh* Clones

Ovarioles are stained as indicated. Clones are marked by the absence of GFP.

(A) *sqh* clones in a wild-type background result in epithelial deformation and outward bulging of the cyst (arrows). Note the size increase of egg chambers between stages 2 and 5.

(B) *sqh* clones in an ovo^{D1} mutant background retain rectangular shape, and the cyst does not bulge outwards. Note that stage 5 and stage 6 egg chambers have the same size, indicating growth arrest.

(C) Magnification of the clones shown in (A) (up) and (C) (down). Arrows compare the apical basal extent of *sqh* mutant and wild-type follicle cells.

The pattern of myosin activity reflects the organization of the actin cytoskeleton. The stress fiber-like pattern at the basal cortex reveals activity in the parallel actin arrays (Figure 1F), and this activity leads to egg-chamber elongation [4, 5]. In contrast to this polarized pattern of myosin, the apical pattern shows no uniform direction, indicating that actin filaments of all orientations contract (Figure 1G). This suggests that the actin filaments at the apical cortex are crosslinked like a net. Thermal fluctuations are higher in actin networks compared to bundled actin filaments [21]. A netlike organization of the actin filaments is therefore consistent with our model, in which myosin-mediated contractions increase cortical stiffness by suppressing thermal fluctuations within the net.

The follicular epithelium responds to the cyst growth by increasing the epithelial surface by cell proliferation. The signal that induces mitosis is unknown. Our data raise the possibility that the actomyosin cytoskeleton is involved in the coordination of cyst growth and epithelial proliferation. It is likely that the apical cortex, which is stiffened by myosin, perceives the volume increase of the growing cyst as a further tension increase in the crosslinked actin filaments. We speculate that tension increase above a certain threshold triggers mitosis in the epithelium. The resulting cell divisions lead to an enlarged epithelial surface and thereby to a tension decrease at the apical cortex. The coupling of tension increase and cell proliferation adapts the growth of the epithelium to the volume increase of the cyst and prevents epithelial rupture. The role of tension in regulating cell growth was proposed in the past [22, 23] and has been demonstrated recently in cell culture experiments [24].

If cyst growth and epithelial proliferation are coupled, follicle cell division should be reduced when the cyst volume does not increase. Notably, we found a dramatic reduction in cell division in ovo^{D1} mutant ovarioles, in which growth is blocked (Table 1). Consistent with this, it has been reported that block of cyst growth induced by germline clones mutant for the *Drosophila Insulin receptor* and *dMyc* does not result in excess follicle cells [25, 26]. These results show that cyst growth and epithelial growth are coupled. However, they allow no conclusion about the coupling mechanism.

The restriction of myosin activity to the apical cortex of the epithelium is mediated by at least three different mechanisms, summarized in Figure S3C. First, myosin phosphorylation at the apical cortex is achieved by apical localization of Rok. Rok is also regulated by the small GTPase Rho1. *rho1* mutant follicle cell clones show reduced apical myosin phosphorylation and cell flattening, suggesting that Rho1 binding enables Rok to phosphorylate myosin. In contrast to *rok* mutant clones, *rho1* mutant cells have large nuclei and an increased cell size, indicating that Rho1 is also required for cytokinesis (data not shown). The second mechanism that restricts myosin activity to the apical cortex is the anchoring of active myosin by the Baz/aPKC/Par-6 complex. The third mechanism is the inhibition of myosin at the lateral and basal cortex via PP1β9C-mediated dephosphorylation. In the future, it will be important to find additional components regulating apical myosin activity, and to find out whether myosin activity is also in other epithelia restricted to certain domains.

Supplemental Data

Experimental Procedures and three figures are available at http://www.current-biology.com/cgi/content/full/17/15/1349/DC1/.

Acknowledgments

Fly stocks and antibodies were kindly provided by L. Alphey, J. Grosshans, R. Karess, J. Knoblich, E. Knust, A. Müller, M. Peifer, A. Wodarz, and the Bloomington stock center. We thank N. Berns, M. Leptin, A. Müller, and S. Roth for comments on the manuscript. This project was supported by the Deutsche Forschungs Gemeinschaft (Sonderforschungsbereich 572). Y.W. is supported by a fellowship by the International Graduate School in Genetics and Functional Genomics in Cologne.

Received: November 20, 2006
Revised: June 27, 2007
Accepted: June 28, 2007
Published online: July 26, 2007

References

1. Spradling, A.C. (1993). Developmental Genetics of Oogenesis (Cold Spring Harbor, New York: Cold Spring Harbor Laboratory Press).
2. Horne-Badovinac, S., and Bilder, D. (2005). Mass transit: Epithelial morphogenesis in the *Drosophila* egg chamber. Dev. Dyn. *232*, 559–574.
3. Gutzeit, H.O. (1990). The microfilament pattern in the somatic follicle cells of mid-vitellogenic ovarian follicles of *Drosophila*. Eur. J. Cell Biol. *53*, 349–356.
4. Bateman, J., Reddy, R.S., Saito, H., and Van Vactor, D. (2001). The receptor tyrosine phosphatase Dlar and integrins organize actin filaments in the *Drosophila* follicular epithelium. Curr. Biol. *11*, 1317–1327.
5. Frydman, H.M., and Spradling, A.C. (2001). The receptor-like tyrosine phosphatase Lar is required for epithelial planar polarity and for axis determination within *Drosophila* ovarian follicles. Development *128*, 3209–3220.
6. Jordan, P., and Karess, R. (1997). Myosin light chain-activating phosphorylation sites are required for oogenesis in *Drosophila*. J. Cell Biol. *139*, 1805–1819.

7. Bresnick, A.R. (1999). Molecular mechanisms of nonmuscle myosin-II regulation. Curr. Opin. Cell Biol. *11*, 26–33.
8. Tanentzapf, G., Smith, C., McGlade, J., and Tepass, U. (2000). Apical, lateral, and basal polarization cues contribute to the development of the follicular epithelium during *Drosophila* oogenesis. J. Cell Biol. *151*, 891–904.
9. Müller, H.A. (2000). Genetic control of epithelial cell polarity: Lessons from *Drosophila*. Dev. Dyn. *218*, 52–67.
10. Abdelilah-Seyfried, S., Cox, D.N., and Jan, Y.N. (2003). Bazooka is a permissive factor for the invasive behavior of discs large tumor cells in *Drosophila* ovarian follicular epithelia. Development *130*, 1927–1935.
11. Benton, R., and St Johnston, D. (2003). *Drosophila* PAR-1 and 14–3-3 inhibit Bazooka/PAR-3 to establish complementary cortical domains in polarized cells. Cell *115*, 691–704.
12. Vereshchagina, N., Bennett, D., Szoor, B., Kirchner, J., Gross, S., Vissi, E., White-Cooper, H., and Alphey, L. (2004). The essential role of PP1beta in *Drosophila* is to regulate nonmuscle myosin. Mol. Biol. Cell *15*, 4395–4405.
13. Amano, M., Ito, M., Kimura, K., Fukata, Y., Chihara, K., Nakano, T., Matsuura, Y., and Kaibuchi, K. (1996). Phosphorylation and activation of myosin by Rho-associated kinase (Rho-kinase). J. Biol. Chem. *271*, 20246–20249.
14. Kimura, K., Ito, M., Amano, M., Chihara, K., Fukata, Y., Nakafuku, M., Yamamori, B., Feng, J., Nakano, T., Okawa, K., et al. (1996). Regulation of myosin phosphatase by Rho and Rho-associated kinase (Rho-kinase). Science *273*, 245–248.
15. Winter, C.G., Wang, B., Ballew, A., Royou, A., Karess, R., Axelrod, J.D., and Luo, L. (2001). *Drosophila* Rho-associated kinase (Drok) links Frizzled-mediated planar cell polarity signaling to the actin cytoskeleton. Cell *105*, 81–91.
16. Edwards, K.A., and Kiehart, D.P. (1996). *Drosophila* nonmuscle myosin II has multiple essential roles in imaginal disc and egg chamber morphogenesis. Development *122*, 1499–1511.
17. Afshar, K., Stuart, B., and Wasserman, S.A. (2000). Functional analysis of the *Drosophila* Diaphanous FH protein in early embryonic development. Development *127*, 1887–1897.
18. Chou, T.B., Noll, E., and Perrimon, N. (1993). Autosomal P[ovoD1] dominant female-sterile insertions in *Drosophila* and their use in generating germ-line chimeras. Development *119*, 1359–1369.
19. Pasternak, C., Spudich, J.A., and Elson, E.L. (1989). Capping of surface receptors and concomitant cortical tension are generated by conventional myosin. Nature *341*, 549–551.
20. Mizuno, D., Tardin, C., Schmidt, C.F., and Mackintosh, F.C. (2007). Nonequilibrium mechanics of active cytoskeletal networks. Science *315*, 370–373.
21. Janmey, P.A., and Weitz, D.A. (2004). Dealing with mechanics: Mechanisms of force transduction in cells. Trends Biochem. Sci. *29*, 364–370.
22. Ingber, D.E., Madri, J.A., and Jamieson, J.D. (1981). Role of basal lamina in neoplastic disorganization of tissue architecture. Proc. Natl. Acad. Sci. USA *78*, 3901–3905.
23. Ingber, D.E., and Jamieson, J.D. (1985). Cells as Tensegrity Structures: Architectural Regulation of Histodifferentiation by Physical Forces Transduced over the Basement Membrane (London: Academic).
24. Nelson, C.M., Jean, R.P., Tan, J.L., Liu, W.F., Sniadecki, N.J., Spector, A.A., and Chen, C.S. (2005). Emergent patterns of growth controlled by multicellular form and mechanics. Proc. Natl. Acad. Sci. USA *102*, 11594–11599.
25. Maines, J.Z., Stevens, L.M., Tong, X., and Stein, D. (2004). *Drosophila* dMyc is required for ovary cell growth and endoreplication. Development *131*, 775–786.
26. LaFever, L., and Drummond-Barbosa, D. (2005). Direct control of germline stem cell division and cyst growth by neural insulin in *Drosophila*. Science *309*, 1071–1073.
27. King, R.C. (1970). Ovarian Development in Drosophila melanogaster (New York: Academic Press).